

# High-Optical-Output-Power and High-Responsivity Integrated Coherent Transmitter-Receiver Optical Sub Assembly for 800 Gbit/s Transmission

Munetaka KUROKAWA\*, Masaru TAKECHI, Yasutaka MIZUNO, Taichi MISAWA, Eiichi BANNO, and Hiroshi HARA

A digital coherent optical transmission technology has been deployed in not only long-haul and metro networks but also data center networks. Therefore, there is an increasing demand for a coherent module that can be incorporated in small-sized optical transceivers and realize high-speed and high-capacity transmission. Considering the demand, the Optical Internetworking Forum has standardized an integrated coherent transmit-receive optical sub assembly (IC-TROSA) module in August 2019. This paper presents an IC-TROSA type-2 module that integrates a tunable laser for 800 Gbit/s applications.

Keywords: coherent optical transmission, IC-TROSA, tunable laser, modulator, photodetector

## 1. Introduction

Internet traffic has been increasing significantly due to the widespread use of social media, video-based content delivery, and IoT communications in line with the commencement of 5G networks. The current challenge is how to respond to this rapid increase in data communications with fiber-optic communication technology.

Digital coherent optical transmission technology increases capacity by transmitting not only the state of optical intensity but also the state of phase as information, thereby carrying more information in a limited band. Digital signals are processed on both the transmitting side and the receiving side to compensate for the degradation of signal quality that occurs in optical fiber transmission, thereby achieving long-distance transmission.

Coherent transmission systems with a transmission speed of 400 Gbit/s have been applied to long-distance networks, such as core/metro networks between large cities. Recently, in order to meet the abovementioned market demand, standardization of coherent transmission corresponding to a transmission speed of 800 Gbit/s has been studied, and deployment of coherent transmission technology between data centers with shorter transmission distances has also been promoted.

In applications for data centers, there are demands for higher transmission speed and smaller coherent modules. Optical Internetworking Forum (OIF),\*<sup>1</sup> an industry standardization organization, formulated a standard for integrated coherent transmit-receive optical sub assembly (IC-TROSA).<sup>\*2</sup> IC-TROSA Type-2<sup>(1)</sup> is a coherent module incorporating three main optical devices (i.e., a tunable laser, a modulator, and a photodetector) and an IC for controlling these devices with a size of W 15.1 mm × L 30.0 mm × H 6.5 mm, which can be mounted in a QSFP-DD<sup>\*3</sup> optical transceiver.<sup>(2)</sup>

Previously, we developed a high-optical-output-power tunable laser module, an optical receiver module,<sup>(3),(4)</sup> and an optical modulator module, and have demonstrated the potential of InP-based devices capable of 400-Gbit/s transmission.

This paper reports a module design and the measured characteristics of a coherent module that complies with the IC-TROSA Type-2 standard and can be used for 800 Gbit/s applications, by integrating the three functions into a single package.

## 2. Configuration of IC-TROSA

Photo 1 shows the appearance of the IC-TROSA we developed. Miniaturization and low profiling have been attained to achieve a package size of W 14.1 mm × L 27.5 mm × H 3.8 mm by using small parts and applying high-integration implementation technology.

A control board, in which ICs are mounted, is arranged at the top of the package and is connected via a flexible printed circuit (FPC) to attain a total module thickness of 6.2 mm so that the design complies with the IC-TROSA Type-2 standard. The control board is equipped

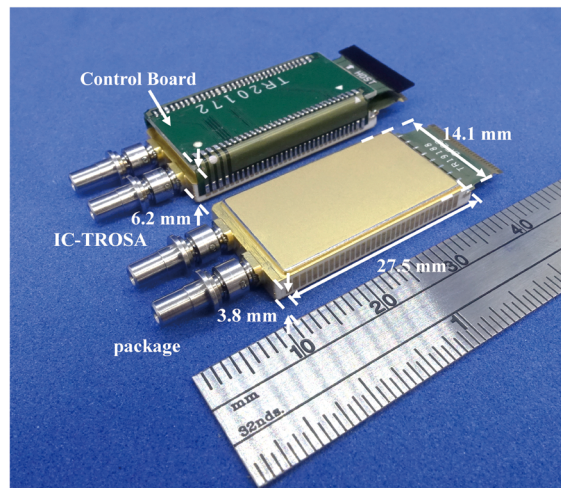


Photo 1. Appearance of IC-TROSA and package

with ICs to supply control voltages and currents to the tunable laser, modulator, and photodetector.

Figure 1 shows a model diagram of the IC-TROSA mounted in the QSFP-DD. The package is sandwiched by a transceiver enclosure at the top and the bottom, and the heat radiation surface of the package is forced to come into contact with the heat radiation surface of the transceiver. In the IC-TROSA, the control board is mounted on the package. Thus, ICs on the control board may become damaged due to pressure from the enclosure. To cope with this problem, metal posts are arranged on the four corners of the package so that the ICs do not come into contact with the package when pressure is applied and so that they can withstand vibration and impacts. The design ensures high reliability and high heat radiation performance.

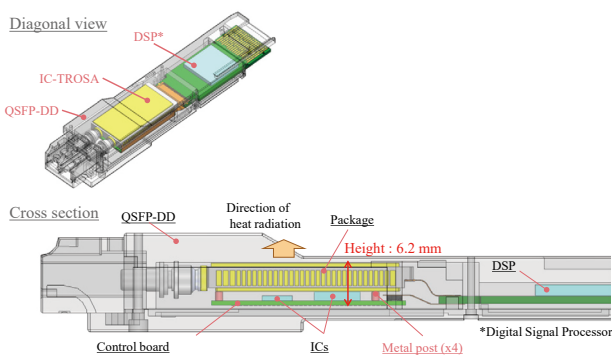


Fig. 1. IC-TROSA mounted in the QSFP-DD

### 3. Module Design

The transmit signals are generated by multiplexing two optical polarization (X-polarization and Y-polarization) signals that are phase modulated by the multi-level encoding modulation method.

The internal configuration of the coherent module is shown in Fig. 2. The coherent module incorporates a tunable laser, a modulator, a photodetector, a driver-IC for

driving the modulator, and a transimpedance amplifier (TIA) for amplifying photodetector output signals. Thermoelectric coolers are also mounted for maintaining the temperatures of the tunable laser and modulator at constant levels.

The arrows in the figure show optical paths among the tunable laser, modulator, and photodetector. The outgoing beam from the tunable laser is separated by the beam splitter (BS) into local light for the photodetector and signal light for the modulator. Part of the light separated to the local light side is further separated into the wavelength control function unit that stabilizes the oscillation wavelength.

Regarding the optical configuration on the transmitting side, the signal light is optically coupled with the modulator, the signal light is separated into four channels in the modulator, and then electrical signals from the driver-IC are converted into optical modulation signals. Two pairs of quadrature-modulated signals are output from the modulator as X-polarization and Y-polarization optical modulation signals. The signals are then combined by the polarization beam combiner (PBC) outside the modulator and output from an optical fiber as modulation signals.

Regarding the optical configuration on the receiving side, the modulation signals input from outside via an optical fiber are separated into X-polarization and Y-polarization by the polarization beam splitter (PBS) and optically coupled with the photodetector. The phase signals are converted into intensity signals in the 90° hybrid optical mixer\*<sup>4</sup> by interference with the local light. The signals are then converted into electric current by the photodiode (PD) corresponding to the four channels for each signal component. Subsequently, the electric current is converted into voltage and amplified by the TIA and demodulated as electrical signals.

To realize a size that complies with the standard, we developed compact and multifunctional integrated semiconductor optical devices. Regarding the modulator, a Mach-Zehnder (MZ) interference\*<sup>5</sup> structure is used. Electrodes are formed in parallel with the optical waveguide, and phase modulation is performed by an electro-optic effect.\*<sup>6</sup> In general, to attain the desired modula-

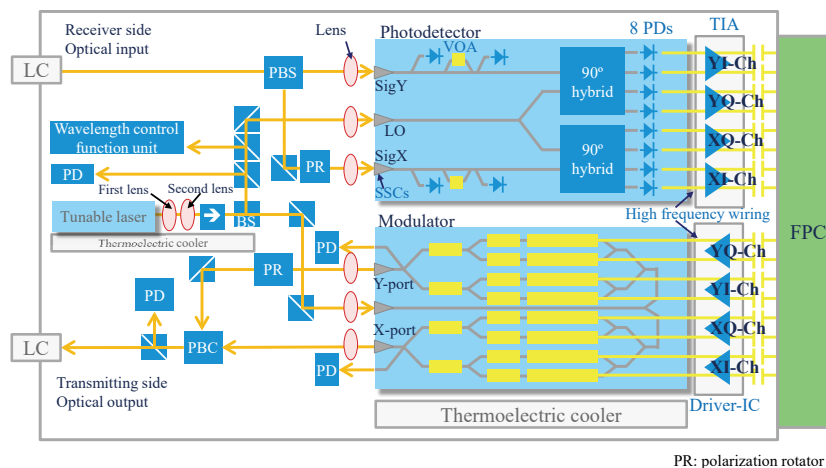


Fig. 2. Configuration in IC-TROSA

tion efficiency, there is a problem that the waveguide lengthens and the size of the device becomes longer. We achieved a compact size of 4.0 mm × 4.4 mm and low-voltage operation by using a structure wherein the waveguide is folded 180° inside the device.<sup>(5)</sup> Regarding the photodetector integrating 90° hybrid optical mixers, a compact size has been achieved by integrating the functions of each part, which are previously implemented as separate parts, in the chip. Specifically, two 90° hybrid optical mixers and eight PDs, four power monitor PDs and two variable optical attenuators (VOAs)\*<sup>7</sup> in each X-port and Y-port input path, are integrated having a size of 2.6 mm × 4.1 mm.<sup>(6),(7)</sup>

For both the modulator and photodetector, a spot-size converters (SSCs)\*<sup>8</sup> are integrated into the input/output ports. The coupling efficiency between the semiconductor optical devices, and also between the fiber and the modulator / the photodetector are improved, and the implementation tolerance during assembly was expanded.

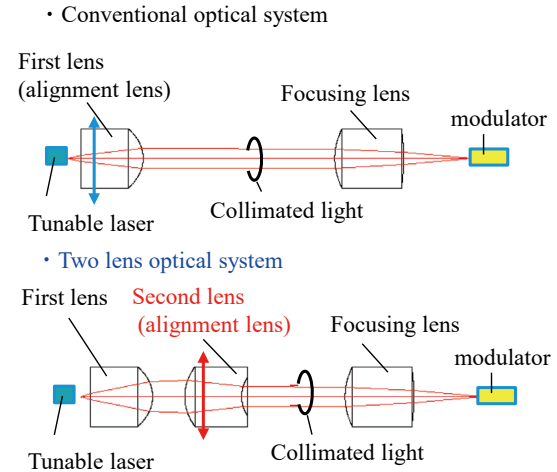
### 4. Optical Characteristic

The tunable laser, modulator, and photodetector are configured using separate semiconductor optical devices. Optical parts, such as the beam splitter, must be mounted between the optical devices. Thus, a spatial optical system is used for optical connection between the optical devices.

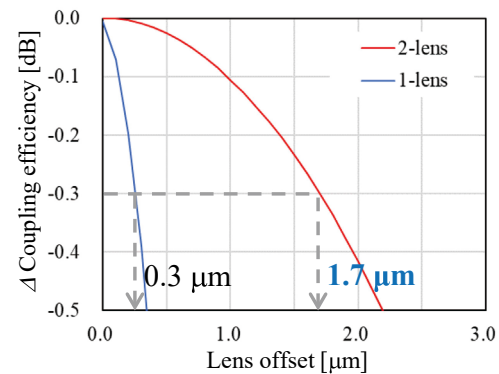
The optical lens system was devised to achieve high optical coupling efficiency between the tunable laser and the modulator. A conventional optical system is shown in the upper part of Fig. 3 (a), wherein the output light from the tunable laser is converted into collimated light by one lens and focused on the modulator using a different lens. However, the tolerance of the lens for the tunable laser is steep, and a problem exists with a reduction of coupling efficiency due to misalignment of the fixed lens. We applied a two-lens optical system as shown in the lower part of Fig. 3 (a). Specifically, the output light of the tunable laser is turned into collimated light by the two-lens configuration. The second lens is used as an alignment lens to flatten the tolerance curve. The results of calculating the tolerance of the alignment lens are shown in Fig. 3 (b). For example, when a lens whose focal distance is six times that of the first lens is used as the alignment lens, the tolerance can also be increased about six times. This effect suppresses the decrease in coupling efficiency when the lens is fixed, and also effective in reducing fluctuations of coupling efficiency against the environment temperature change of the package.

In Fig. 4, the optical output power of X-polarization and Y-polarization from IC-TROSA and the total optical output power are plotted on the primary axis. The wavelength dependence of the difference in optical output power of X-polarization and Y-polarization (PDL) is plotted on the secondary axis. A tunable laser<sup>(8)</sup> that has a narrow linewidth and a high optical output power was used as the light source. The operating condition was 210 mA for the laser diode (LD) electric current and 250 mA for the SOA\*<sup>9</sup> electric current. Each MZ of the modulator was biased at the maximum light transmission condition. The maximum optical output power was 9.2 dBm. The optical output

power was high for both X-polarization and Y-polarization (6 dBm or higher). In the case of transmission based on the 32 QAM\*<sup>10</sup> modulation format, output of -6.0 dBm or more is expected with a modulation loss of 13 dB.



(a) Optical configuration between tunable laser and modulator



(b) Comparison of lens tolerance

Fig. 3. Optical system between tunable laser and modulator

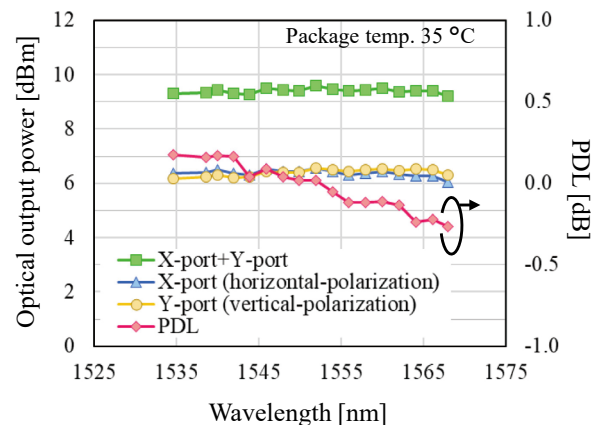


Fig. 4. Optical output power on the transmitting side and difference between the X-polarization and the Y-polarization

Figure 5 shows the wavelength dependence of responsivities of the signal lights (Sig-X/Y) at a package temperature of 35°C. The voltage applied to the PD was 5 V, and the TIA power supply voltage was 3.3 V. A responsivity of 62 mA/W or more was attained at a wavelength of 1550 nm. The deviation between the channels was confirmed to be ±0.3 dB or less.

The package temperature characteristics of the sensitivity of the signal lights and local light (LO) are shown in Fig. 6. Variations of sensitivity of ±0.3 dB or less were obtained within a temperature range between -5°C and 75°C.

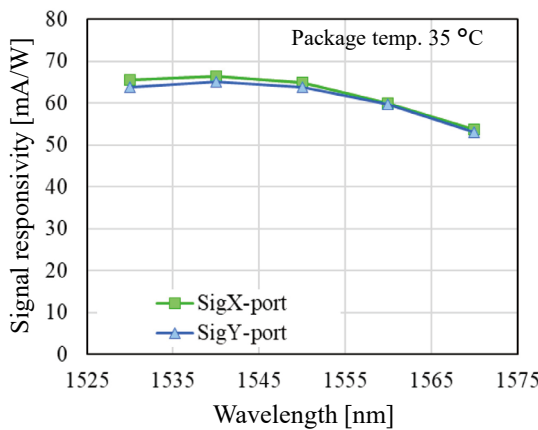


Fig. 5. Wavelength dependence of signal sensitivity

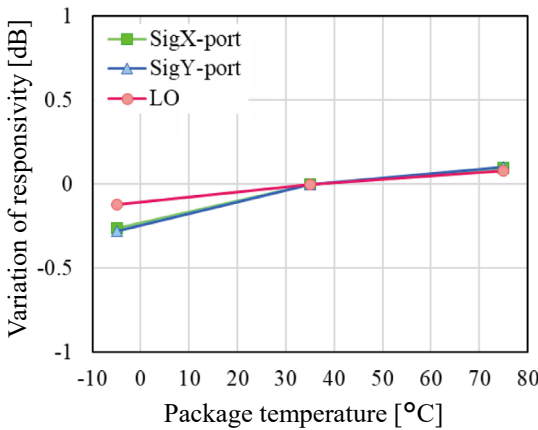


Fig. 6. Temperature dependence of Signal and LO sensitivity variation

### 5. Frequency Response Characteristics

The frequency response depends on the performance of the semiconductor optical device to be mounted, the characteristics of the driver-IC and TIA, and the high-frequency design between the FPC and the package, between the package and the driver-IC, and between the package and the TIA. We obtained good characteristics over a wide bandwidth of 50 GHz or more by optimizing the characteristics based on combinations of the optical devices and driver-IC/TIA and adjusting the overall impedance in the

high-frequency design.

Figure 7 shows the measurement results of the electrical-optical (E/O) frequency response on the transmitting side of each channel. A 3 dB band of 57 GHz was attained, which is capable for 800 Gbit/s operation, and flat characteristics were obtained from low to high frequency.

The measurement results of optical-electrical (O/E) frequency response for a specific channel (XI) as a

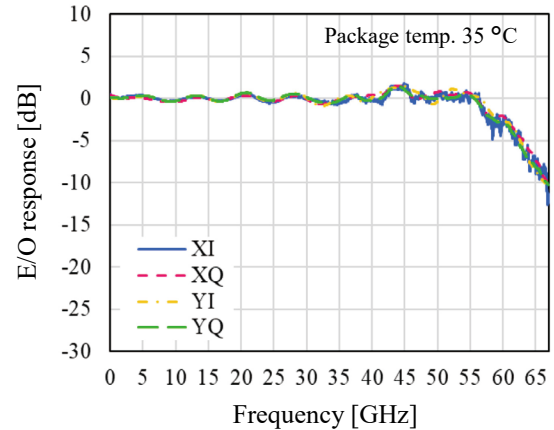


Fig. 7. Frequency response characteristics on the transmitting side

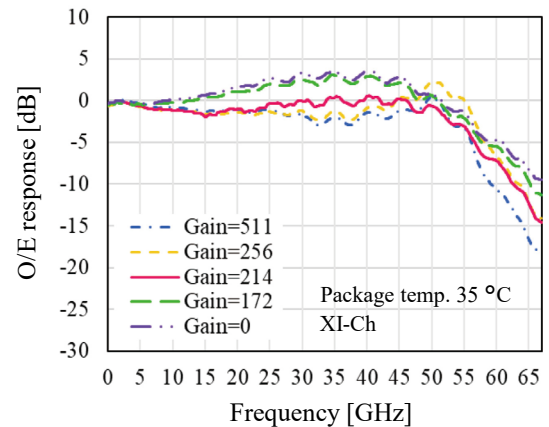


Fig. 8. Frequency response characteristics on the receiving side

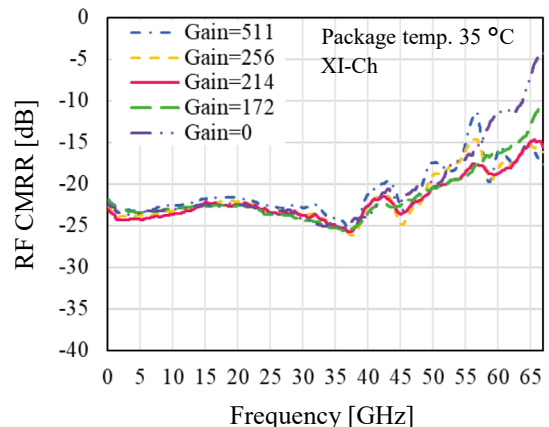


Fig. 9. CMRR during modulation

function of TIA gain setting (from 0 to 511) are shown in Fig. 8. A 3 dB bandwidth of 55 GHz was attained at the optimum value of the TIA setting. In the photodetector, demodulation signals are affected by the mixing of common-mode signals with differential signals. Thus, a high common-mode rejection ratio (CMRR) is required. As shown in Fig. 9, a CMRR of  $-15$  dB or less were confirmed up to 55 GHz by optimizing the high-frequency design.

## 6. Conclusion

We have developed a module that complies with the IC-TROSA Type-2 standard by integrating the tunable laser, modulator, photodetector, thermoelectric cooler, and driver-IC for driving the modulator, and TIA for the photodetector into a single package with a size of W 14.1 mm  $\times$  L 27.5 mm  $\times$  H 3.8 mm.<sup>(9)</sup>

A 3 dB bandwidth of more than 55GHz, which supports a transmission speed of 800 Gbit/s with a 32QAM modulation format, was confirmed both on the transmitting side and the receiving side, achieving high optical output power and high sensitivity.

We believe that this module contributes to smaller-sized and higher-speed digital coherent optical transceivers, and realization of an optical communication system that will underpin the post-5G era.

### Technical Terms

- \*1 Optical Internetworking Forum (OIF): An industry organization on optical network technology that promotes standardization.
- \*2 Integrated Coherent Transmit-Receive Optical Subassembly (IC-TROSA): A coherent communication module that integrates both receiving and transmitting functions. There are two types: Type 1 and Type 2. In Type 1, the tunable laser is installed outside the module. In Type 2, the tunable laser is installed inside the module.
- \*3 Quad Small Form-factor Pluggable-Double Density (QSFP-DD): The transceiver size is 72.4 mm  $\times$  18.4 mm  $\times$  8.5 mm.
- \*4 90° hybrid optical mixer: A mechanism that outputs in-phase components and quadrature components by interfering the signal light with local light in the coherent receiver.
- \*5 Mach-Zehnder (MZ) interference: A waveguide structure to distribute light by using multi-mode interference, which occurs in the waveguide.
- \*6 Electro-optic effect: A nonlinear optical phenomenon. This is a technology using changes in the refractive index when a voltage is applied.
- \*7 Variable Optical Attenuator (VOA): A function to adjust the input/output light intensity.
- \*8 Spot-Size Converter (SSC): A waveguide structure whose function is to convert the mode field diameter.
- \*9 Semiconductor Optical Amplifier (SOA): A Semiconductor element that amplifies the input light intensity by stimulated emission.
- \*10 Quadrature Amplitude Modulation (QAM): A method for modulating two in-phase and quadrature amplitudes that are independent from each other.

### References

- (1) "Implementation Agreement for Integrated Coherent Transmit-Receive Optical Sub Assembly," <https://www.oiforum.com/wp-content/uploads/OIF-IC-TROSA-01.0.pdf> (August, 2019)
- (2) "QSFP-DD MSA," <http://www.qsfp-dd.com/>
- (3) M. Takechi, Y. Tateiwa, M. Kurokawa, Y. Fujimura, H. Yagi, and Y. Yoneda, "64 GBaud High-bandwidth Micro Intradyn Coherent Receiver Using High-efficiency and High-speed InP-based Photodetector Integrated with 90° Hybrid," OFC2017, paper Th1A.2 (2017)
- (4) M. Kurokawa, M. Takechi, H. Yagi, K. Sakurai, Y. Yoneda, and Y. Fujimura, "High-responsivity L-band micro intradyne coherent receiver using InP-based photodetector integrated with 90-degree hybrid," Photonics West2018, vol. 10561, paper 1056105. doi (2018)
- (5) H. Tanaka, T. Ishikawa, T. Kitamura, M. Watanabe, R. Yamabi, R. Yamaguchi, N. Kono, T. Kikuchi, M. Seki, T. Katsuyama, M. Ekawa, and H. Shoji, "Highly Reliable and Compact InP-Based In-Phase and Quadrature Modulators for Over 400 Gbit/s Coherent Transmission Systems," IEICE Transactions on electronics, Vol. E103-C, No.11, pp. 661-668 (July, 2020)
- (6) H. Yagi, T. Okimoto, N. Inoue, K. Ebihara, K. Sakurai, M. Kurokawa, S. Okamoto, K. Horino, T. Takeuchi, K. Yamazaki, Y. Nishimoto, Y. Yamasaki, M. Ekawa, M. Takechi, and Y. Yoneda, "InP-Based Photodetectors Monolithically Integrated with 90° Hybrid toward Over 400 Gb/s Coherent Transmission Systems," IEICE Transactions on electronics, Vol.E102-C, No.4, pp. 347-356 (Apr, 2019)
- (7) T. Okimoto, H. Yagi, K. Ebihara, K. Yamazaki, S. Okamoto, Y. Ohkura, K. Horino, K. Ashizawa, M. Ekawa, and Y. Yoneda, "InP-based PIC integrated with Butt-joint Coupled Waveguide p-i-n PDs for 100GBaud Coherent Networks," OFC2021, paper F2C.6 (2021)
- (8) T. Kaneko, Y. Yamauchi, K. Uesaka, and H. Shoji, "A Single-Stripe Tunable Laser Operated at Constant Temperature Using Thermo-Optic Effect," 17th MOC, paper G-25 (Oct, 2011)
- (9) M. Kurokawa, K. Nakayama, M. Takechi, Y. Mizuno, T. Misawa, E. Banno, H. Uemura, Y. Sugimoto, S. Kumagai, T. Okimoto, N. Kono, T. Ishikawa, H. Hara, T. Kato, K. Tanaka, M. Ekawa, and K. Uesaka, "High Optical Output Power and High-responsivity IC-TROSA for 800 Gbps applications," ECOC2021, paper We4.G.1 (2021)

---

**Contributors** The lead author is indicated by an asterisk (\*).

**M. KUROKAWA\***

• Assistant Manager, Transmission Devices Laboratory



**M. TAKECHI**

• Senior Assistant General Manager, Transmission Devices Laboratory



**Y. MIZUNO**

• Transmission Devices Laboratory



**T. MISAWA**

• Transmission Devices Laboratory



**E. BANNO**

• Assistant General Manager, Transmission Devices Laboratory



**H. HARA**

• Senior Assistant General Manager, Transmission Devices Laboratory

